Atmospheric
Chemistry
and Physics

Supplement of

The importance of moist thermodynamics on neutral buoyancy height for plumes from anthropogenic sources

Sepehr Fathi et al.

Correspondence to: Sepehr Fathi (sepehr.fathi@ec.gc.ca)

S1 PRISM (Plume-Rise-Iterative-Stratified-Moist) and Discrete Numerical Formulations

The input stack parameters include stack-top height z_{stack} in meters [m] agl (above ground level), stack radius r_{stack} [m], stack volume flow rate $\dot{V}_{stack}$ [m^3/s], stack/effluent temperature T_{stack} [K], effluent exit velocity w_{stack} [m/s], and stack water/vapour emission rate E_{H_2O} [kg/s].

5   As a first step, dry air density of the effluent at stack top (level $j = 0$) is calculated using the ideal gas law,

$$\rho_{d,0} = \frac{P_{a,0}}{k\,T_{stack}} \tag{S1}$$

where $P_{a,0}$ [Pa] is the ambient air pressure at stack-top, and $k = 287$ [J kg^{-1}K^{-1}] is the gas constant for dry air.

    Parcel initial volume during time Δt_0 after release can be calculated using the stack volume flow rate,

$$V_0 = \dot{V}_{stack}\,\Delta t_0 \quad [\text{m}^3] \tag{S2}$$

10 Similarly, the amount of water vapour released during the same time can be calculated from the known stack/source emission rate for water

$$M_{H_2O,0} = E_{H_2O}\,\Delta t_0 \quad [\text{kg}] \tag{S3}$$

    The parcel initial vapour mixing ratio is then calculated as,

$$q_{v,0} = \frac{M_{H_2O,0}}{\rho_{d,0}\,V_0} \tag{S4}$$

15 Which can be used to estimate the parcel density (a mixture of air and vapour) using the ideal gas law (Rogers and Yau, 1989),

$$\rho_0 = \frac{P_{a,0}}{k\,T_{v,stack}} \tag{S5}$$

where stack virtual temperature is $T_{v,stack} = T_{stack}\left(1 + q_{v,0}/\varepsilon\right)/\left(1 + q_{v,0}\right) \approx T_{v,stack}\left(1 + 0.61 q_{v,0}\right)$.

    Buoyancy flux at the stack top is defined as the product of buoyant acceleration and the volume flow rate,

20
$$F_0 = \left(g\,\frac{\rho_a - \rho_0}{\rho_0}\right)\dot{V}_{stack} \tag{S6}$$

where g is the gravitational acceleration, and ρ_a [kg/m^3] is the ambient air density.

    The entrained volume flux at level j for the vertical and the bent-over models are calculated following the formulations by Briggs (1984),

$$\dot{V}_j = \begin{cases} 0.791\,\alpha^{4/3}\,F_0^{1/3}\,\acute{z}_j^{5/3} & [\text{m}^3\text{/s}], \quad \text{vertical.} \\ \pi\,U_j\beta^2\,\acute{z}_j^2 & [\text{m}^3\text{/s}], \quad \text{bent-over.} \end{cases} \tag{S7}$$

25 where $\acute{z} = z_{j+1} - z_{stack}$ is the height above stack. The empirical entrainment coefficients for buoyant plumes recommended by Briggs (1984) are $\alpha = 0.08$ and $\beta = 0.6$ for vertical and bent-over plumes, respectively. Equation (S7) gives the rate of change in parcel volume due to entrainment.

The buoyant acceleration at each model vertical level due to density difference between the plume parcel and the ambient air is calculated as

$$\widetilde{a}_j = g \, \frac{\rho_a - \rho_j}{\rho_j} \quad [\text{m/s}^2] \tag{S8}$$

from which the transit time between levels j and $j+1$ can be derived,

$$\Delta t = \frac{-(w_j) + \sqrt{w_j^2 + 2\widetilde{a}_{j+1}\Delta z_{j+1}}}{\widetilde{a}_{j+1}} \quad [\text{s}] \tag{S9}$$

where w_j [m/s] is parcel upwards velocity at level j, and Δz_{j+1} [m] is the height difference between levels j and $j+1$. Further we calculate the change in volume over time Δt using the average volume flux between levels j and $j+1$,

$$\Delta V_{j+1} = \frac{1}{2}\left(\dot{V}_{j+1} + \dot{V}_j\right)\Delta t \quad [\text{m}^3] \tag{S10}$$

which can be used to calculate parcel volume at level $j+1$: $V_{j+1} = V_j + \Delta V_{j+1}$. The mass of ambient air entrained from the surrounding atmosphere into the rising plume as it rises from vertical level j to $j+1$ $\Delta m_{j+1} = \Delta(\rho_{a,j+1} V_{j+1})$ is thus,

$$\Delta m_{j+1} = \begin{cases} 0.791\,\alpha^{4/3}\,F_0^{1/3}\left(\rho_{a,j+1}z_{j+1}^{5/3} + \rho_{a,j}z_j^{5/3}\right)\frac{\Delta t}{2} & [\text{kg}], \text{ vertical.} \\ \pi\beta^2\left(\rho_{a,j+1}U_{j+1}z_{j+1}^2 + \rho_{a,j}U_j z_j^2\right)\frac{\Delta t}{2} & [\text{kg}], \text{ bent-over.} \end{cases} \tag{S11}$$

This entrained air mass can be used to determine two additional heat transfer terms. When the entrained air is added to the parcel, heat must be added to the entrained air to bring it to the same temperature as the parcel (i.e. the heat must be removed from the parcel to the entrained air):

$$\Delta Q_{en,j+1} = -\,C_p\left(T_{j+1} - T_{a,j+1}\right)\Delta m_{j+1} \tag{S12}$$

so for the vertical plume we get

$$\Delta Q_{en,j+1} = -\,0.791\,C_p\,\alpha^{4/3}\,F_0^{1/3}\left(T_{j+1} - T_{a,j+1}\right)\left(\rho_{a,j+1}z_{j+1}^{5/3} + \rho_{a,j}z_j^{5/3}\right)\frac{\Delta t}{2} \tag{S13}$$

and similarly for the bent-over plume

$$\Delta Q_{en,j+1} = -\,C_p\pi\beta^2\left(T_{j+1} - T_{a,j+1}\right)\left(\rho_{a,j+1}U_{j+1}z_{j+1}^2 + \rho_{a,j}U_j z_j^2\right)\frac{\Delta t}{2} \tag{S14}$$

causing the corresponding change (decrease) in parcel temperature at level $j+1$,

$$\Delta T_{en,j+1} = \frac{\Delta Q_{en,j+1}}{M\,C_p} \tag{S15}$$

where T_{j+1} and $T_{a,j+1}$ are parcel and ambient air temperatures in kelvin [K] at level $j+1$, respectively. $C_p = 1004$ [J kg^{-1} K^{-1}] is specific heat at constant pressure, and $M = \rho\,V$ is the total parcel mass in kilograms [kg].

A final consideration with regards to entrainment is that the parcel may be rising through air which contains water, in both gaseous and liquid form, and this water may be entrained during the rise from level j to level $j + 1$. With $q_{c,a}$ and $q_{v,a}$ as the ambient condensed and vapour phase water mass mixing ratios, the total mass of water gained via entrainment between levels j and $j + 1$ will be:

$$\Delta m_{\mathrm{H_2O}} = \int_j^{j+1} (q_{v,a} + q_{c,a})\, dm \approx \frac{1}{2} (q_{v,a,j} + q_{c,a,j} + q_{v,a,j+1} + q_{c,a,j+1})\, \Delta m_{j+1} = \Delta m_{\mathrm{H_2O},v} + \Delta m_{\mathrm{H_2O},c} \tag{S16}$$

Where $\Delta m_{\mathrm{H_2O},v}$ and $\Delta m_{\mathrm{H_2O},c}$ are entrained water mass in vapour/gas and condensed/liquid phase, respectively. The total mass of water added to the parcel due to entrainment for the vertically rising plume is thus:

$$\Delta m_{\mathrm{H_2O}} = \frac{1}{2} (q_{v,a,j} + q_{c,a,j} + q_{v,a,j+1} + q_{c,a,j+1}) \left[0.791\, \alpha^{4/3}\, F_0^{1/3} \left(\rho_{a,j+1} z_{j+1}^{5/3} + \rho_{a,j} z_j^{5/3} \right) \frac{\Delta t}{2} \right] \tag{S17}$$

Similarly, the total mass of water added to the parcel due to entrainment for the bent-over plume is:

$$\Delta m_{\mathrm{H_2O}} = \frac{1}{2} (q_{v,a,j} + q_{c,a,j} + q_{v,a,j+1} + q_{c,a,j+1}) \left[\pi \beta^2 \left(\rho_{a,j+1} U_{j+1} \acute{z}_{j+1}^2 + \rho_{a,j} U_j \acute{z}_j^2 \right) \frac{\Delta t}{2} \right] \tag{S18}$$

Which leads to within-parcel net water mass of

$$m_{\mathrm{H_2O},j+1} = m_{\mathrm{H_2O},j} + \Delta m_{\mathrm{H_2O}} \qquad \text{or,} \qquad m_{\mathrm{H_2O},j+1} = m_{\mathrm{H_2O},j} + (\Delta m_{\mathrm{H_2O},v} + \Delta m_{\mathrm{H_2O},c}) \tag{S19}$$

at level $j + 1$. Where $m_{\mathrm{H_2O},j}$ is water mass at level j, with $m_{\mathrm{H_2O},0}$ equal to the mass of the emitted water at stack top. We calculate the equivalent vapour pressure for the net amount of water in the parcel as

$$e_{v,j+1} = \frac{1}{\varepsilon} P_{a,j+1} \left(\frac{m_{\mathrm{H_2O},j+1}}{\rho_{d,j+1} V_{j+1}} \right) = \frac{1}{\varepsilon} k T_{j+1} \left(\frac{m_{\mathrm{H_2O},j+1}}{V_{j+1}} \right) \tag{S20}$$

Note that we used the ideal gas law for dry air (see Eq. S1) to also write the expression in terms of temperature T_{j+1}. Also, note that Eq. (S20) can result in a vapour pressure that is above saturation; the point of using the net (gas + liquid) water concentration ($q_{c,a}$ and $q_{v,a}$) in Eq. (S20) is to determine the water vapour which must be in the condensed phase. If the parcel temperature drops below the saturation temperature at a given level, the amount of water mass mixing ratio present in the condensed phase can be derived from the excess vapour pressure above saturation. From Iribarne and Godson (1981), the saturation vapour pressure of water in [Pa] as a function of temperature in [K] is given by:

$$e_{sat}(T) = 10^{[-2937.4/T - 4.9283\, log_{10}T + 25.5471]} \tag{S21}$$

the condensed water is then calcualted as follows,

$$q_{c\,j+1} = max \left[\left(\frac{1}{\varepsilon} k T_{j+1} \left(\frac{m_{\mathrm{H_2O},j+1}}{V_{j+1}} \right) - e_{sat}(T_{j+1}) \right) \frac{\varepsilon}{P_{a\,j+1}}, \, 0.0 \right] \tag{S22}$$

The consequent change in parcel liquid water mass, results in latent heat release/uptake,

$$\Delta Q_{cond,j+1} = L_v \left[\rho_{d,j+1}\, V_{j+1}\, q_{c_{j+1}} - \left(\rho_j\, V_j\, q_{c_j} + \Delta m_{\mathrm{H_2O},c} \right) \right] \tag{S23}$$

and the corresponding change in parcel temperature

$$\Delta T_{cond,j+1} = \frac{\Delta Q_{cond}}{M\, C_p} = \frac{L_v}{(\rho_{d,j+1}\, V_{j+1})\, C_p} \left[\rho_{d,j+1}\, V_{j+1}\, q_{c_{j+1}} - \left(\rho_j\, V_j\, q_{c_j} + \Delta m_{\mathrm{H_2O},c} \right) \right] \tag{S24}$$

where L_v is the latent heat of condensation. Note that by including both the level j condensed water mass ($\rho_j V_j q_{c_j}$) and the entrained liquid water mass ($\Delta m_{\mathrm{H_2O},c}$) in Eq. (S24), we are accounting for both evaporation of the preexisting (within plume) liquid water and the evaporation of the entrained liquid water. In this formulation, in addition to latent heating, the evaporation of condensed/liquid water can result in latent cooling.

Next, we drive the change in parcel/plume temperature due to entrainment/expansion and phase changes of water. For each case, vertical or bent-over plume, we substitute the appropriate terms from Eqs. (S6)-(S24) into the following expression,

$$\Delta T_{j+1} = \Delta T_{en,j+1} + \Delta T_{cond,j+1} = \frac{1}{M \, C_p} \left[\Delta Q_{en,j+1} + \Delta Q_{cond,j+1} \right] \tag{S25}$$

Thus for the Vertical plume case we get,

$$\Delta T_{j+1} = \frac{1}{\rho_{d,j+1} V_{j+1}} \left[\frac{L}{c_p} \left(\rho_{d,j+1} V_{j+1} q_{cj+1} - \rho_j V_j q_{cj} - \Delta m_{\mathrm{H_2O},c} \right) \right]$$
$$- \frac{1}{\rho_{d,j+1} V_{j+1}} \left[0.79 \alpha^{4/3} F_0^{1/3} \frac{\Delta t}{2} \left(T_{j+1} - T_{a,j+1} \right) \left(\rho_{a,j+1} \dot{z}_{j+1}^{5/3} + \rho_{a,j} \dot{z}_j^{5/3} \right) \right] \tag{S26}$$

to be solved iteratively. To simplify the derivations that follow we collect the terms as,

$$A = \left(\rho_{aj+1} \dot{z}_{j+1}^{5/3} + \rho_{aj} \dot{z}_j^{5/3} \right) \tag{S27}$$

$$B = 0.7914 \alpha^{4/3} F_0^{1/3} \frac{\Delta t}{2} \, T_{a,j+1} \tag{S28}$$

$$C = -0.7914 \alpha^{4/3} F_0^{1/3} \frac{\Delta t}{2} \, A \tag{S29}$$

Similarly, for the Bent-over plume case we get

$$\Delta T_{j+1} = \frac{1}{\rho_{d,j+1} V_{j+1}} \left[\frac{L}{c_p} \left(\rho_{d,j+1} V_{j+1} q_{cj+1} - \rho_j V_j q_{cj} - \Delta m_{\mathrm{H_2O},c} \right) \right]$$
$$- \frac{1}{\rho_{d,j+1} V_{j+1}} \left[\pi \beta^2 \frac{\Delta t}{2} \left(T_{j+1} - T_{a,j+1} \right) \left(\rho_{a,j+1} U_{j+1} \dot{z}_{j+1}^2 + \rho_{a,j} U_j \dot{z}_j^2 \right) \right] \tag{S30}$$

and collecting terms as,

$$A = \left(\rho_{a,j+1} U_{j+1} \dot{z}_{j+1}^2 + \rho_{a,j} U_j \dot{z}_j^2 \right) \tag{S31}$$

$$B = \pi \beta^2 \frac{\Delta t}{2} \, T_{a,j+1} \tag{S32}$$

$$C = -\pi \beta^2 \frac{\Delta t}{2} \, A \tag{S33}$$

which will be solved iteratively in the next step. Further, we collect the latent heat related terms in a dummy variable Λ_{j+1}, to use in the subsequent derivations, as follows

$$\Lambda_{j+1} \left(T_{j+1}^n \right) = \begin{cases} \frac{\varepsilon \, L\left(T_{j+1}^n\right)}{c_p P_{a\,j+1}}, & \text{if } \frac{1}{\varepsilon} k T_{j+1} \left(\frac{m_{H2O\,j+1}}{V_{j+1}} \right) > e_{sat} \left(T_{j+1} \right) \\ 0, & \text{if } \frac{1}{\varepsilon} k T_{j+1} \left(\frac{m_{H2O\,j+1}}{V_{j+1}} \right) \le e_{sat} \left(T_{j+1} \right). \end{cases} \tag{S34}$$

with its derivative with respect to T_{j+1}

$$\Lambda'_{j+1} \left(T_{j+1}^n \right) = \frac{\varepsilon \, L' \left(T_{j+1}^n \right)}{c_p P_{a\,j+1}} \tag{S35}$$

4

To find T_{j+1}, we solve Eqs. (S26) and (S30) (with their corresponding A, B, C terms) using the Newton-Raphson method (Oxford, 2014) as following: we collect all the terms in Eqs. (S26) or (S30) on one side of the equilibrium and label it as F,

$$
\begin{aligned}
F = {} & T_{j+1}^n - T_j - \Lambda_{j+1}\left(T_{j+1}^n\right)\left(\frac{1}{\varepsilon}\, kT_{j+1}^n\, \frac{m_{H2Oj+1}}{V_{j+1}} - e_{sat}\left(T_{j+1}^n\right)\right) \\
& - \frac{kT_{j+1}^n}{P_{aj+1}V_{j+1}}\left(-\frac{L}{c_p}(\rho_j V_j q_{cj} + \Delta m_{\mathrm{H_2O},c}) + AB + CT_{j+1}^n\right) = 0
\end{aligned}
\tag{S36}
$$

then we take the derivative of F with respect to T_{j+1}^n

$$
\begin{aligned}
F' = {} & 1 - \Lambda'_{j+1}\left(\frac{1}{\varepsilon}\, kT_{j+1}^n\, \frac{m_{H2Oj+1}}{V_{j+1}} - e_{sat}\left(T_{j+1}^n\right)\right) - \Lambda_{j+1}\left(\frac{1}{\varepsilon}\, k\frac{m_{H2Oj+1}}{V_{j+1}} - e_{sat}{'}_{j+1}\right) \\
& - \frac{k}{P_{aj+1}V_{j+1}}\left(-\frac{L}{c_p}(\rho_j V_j q_{cj} + \Delta m_{\mathrm{H_2O},c}) + AB + CT_{j+1}^n\right) - \frac{kT_{j+1}^n}{P_{aj+1}V_{j+1}}\left(-\frac{L'}{c_p}(\rho_j V_j q_{cj} + \Delta m_{\mathrm{H_2O},c}) + C\right)
\end{aligned}
\tag{S37}
$$

Finally, we use the ratio F/F' to adjust the temperature at level $j+1$ at each iteration,

$$
T_{j+1}^{n+1} = T_{j+1}^n - \frac{F}{F'}
\tag{S38}
$$

where T_{j+1}^n and T_j^n are temperature at levels $j+1$ and j at nth iteration, respectively.

In our algorithm, the iterative solution terminates when the subsequent calculated change in temperature at each iteration $(T_{j+1}^{n+1} - T_{j+1}^n)$ becomes smaller than a user specified threshold (e.g., 10^{-6} K). At which point T_{j+1}^{n+1} will be set as parcel equilibrium temperature at level $j+1$.

The updated temperature is then used to re-calculate parcel density,

$$
\rho_{j+1} = \frac{P_{a,j+1}}{k\, T_{j+1}(1 + 0.61 q_{v,j+1} - q_{c,j+1})}
\tag{S39}
$$

Next, parcel density is compared to ambient air density to determine whether the parcel is still buoyant, in which case it will rise to the next layer up and all the above calculations repeat at the new vertical level. This process continues until parcel density approaches the ambient air density, resulting in zero or negative buoyancy. When the normalized difference between parcel and ambient air density falls below a user defined threshold (e.g., $\rho_{conv} = 3 \times 10^{-3}$), parcel is not considered buoyant anymore and the rise terminates.

The vertical level at which rise terminates is then used as the plume final/equilibrium height Δh above the stack. Finally, the plume vertical spread is determined from the plume rise above the stack-top (Δh) and the emitted mass of the pollutants are uniformly distributed in the vertical between plume bottom and top determined following the commonly used method from Briggs (1975),

$$
\begin{aligned}
h_t &= h_s + 1.5\,\Delta h, \\
h_b &= h_s + 0.5\,\Delta h,
\end{aligned}
\tag{S40}
$$

where h_s, h_t and h_b are stack top, plume top and plume bottom heights, respectively.
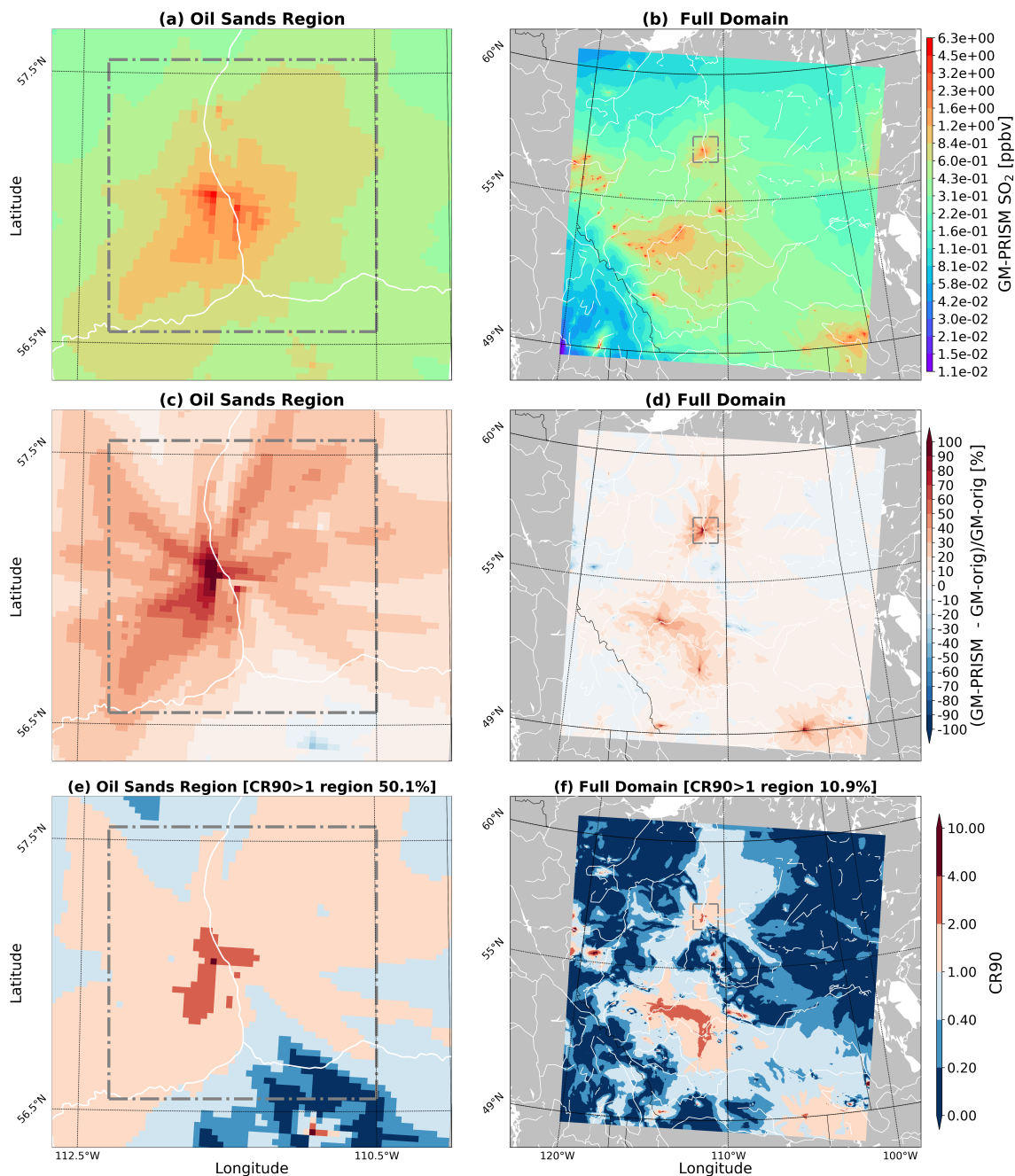
Figure S1. Average surface SO_2 concentrations for the wintertime period (February, March, April of 2018) generated by GM-PRISM simulations shown for (a) oil sands region and (b) the entire domain. (c,d) normalized mean bias (NMB) in % relative to GM-orig simulations for the same period. (e,f) confidence ratio at 90% confidence level (CR90).
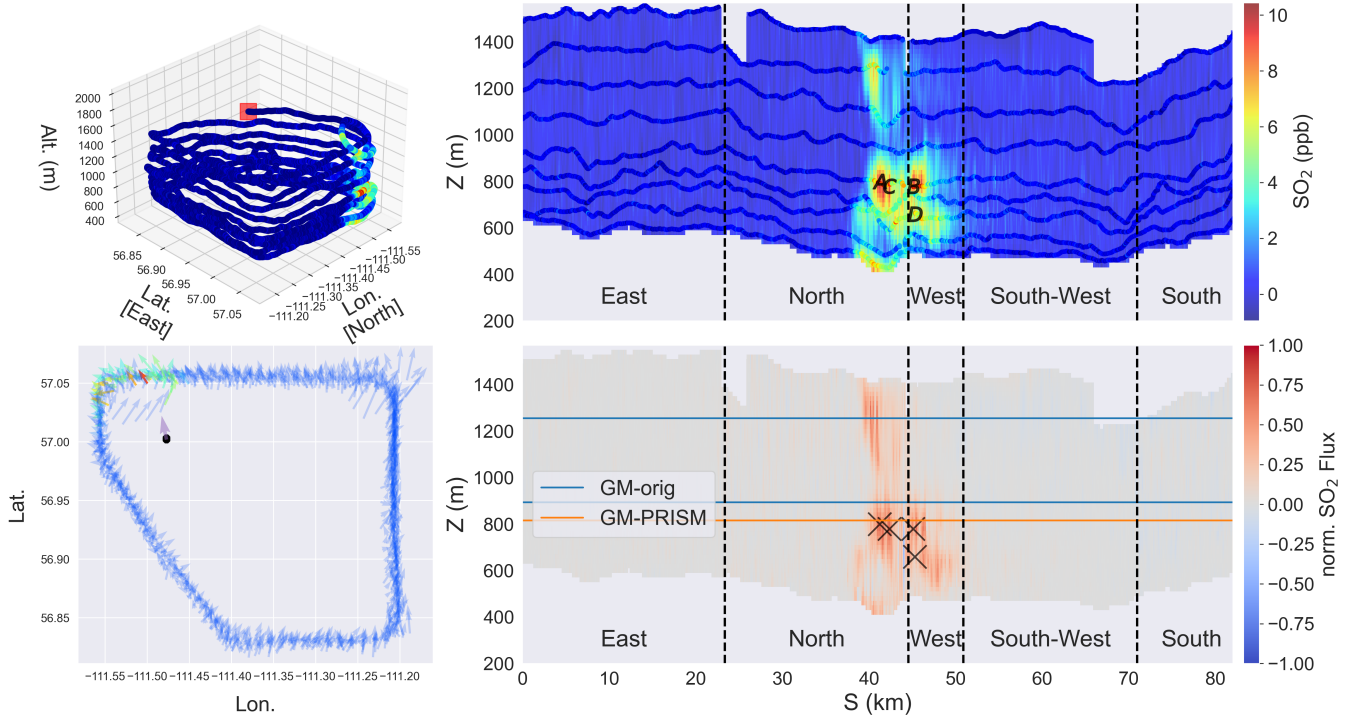
Figure S2. SO$_2$ plume heights were determined from interpolated aircraft concentration measurements. On the left, aircraft concentration (top) and wind data (bottom) along the flight tracks are shown. On the right, the interpolated concentration (top) and normalized mass flux (bottom) data are shown. Plume height predictions by GM-orig and GM-PRISM for this case (Flight 11, Suncor) are overlaid on the flux screen.
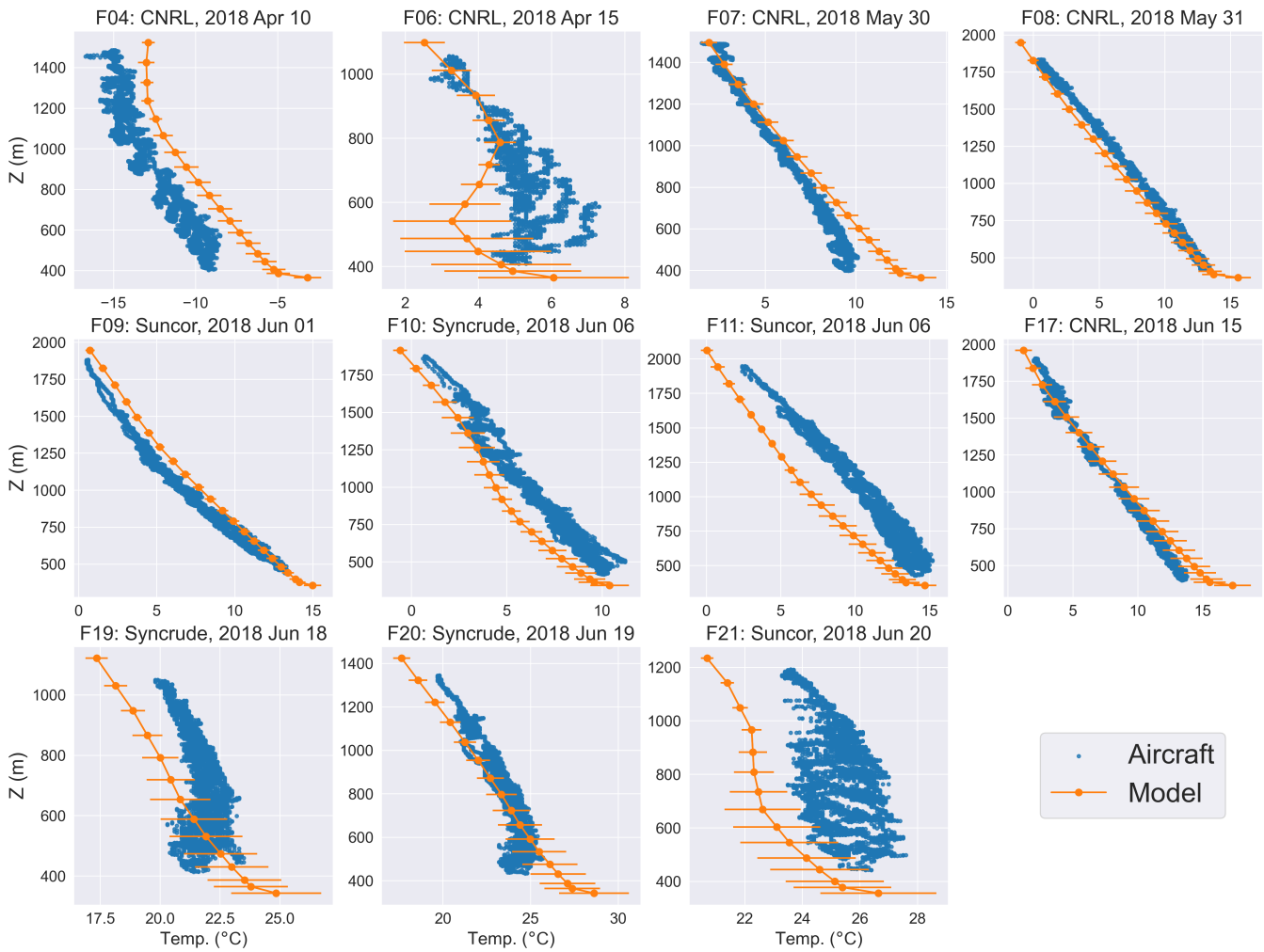
Figure S3. Model generated temperature profiles compared to aircraft observations (blue dots) for the eleven case studies. The horizontal bars indicate the variation in model temperatures over the oil sands facility of interest and over time. For Flight 04 on 10 April 2018, model temperatures showed a consistent positive bias (at all heights) compared to aircraft measurements. Using aircraft-observed temperatures for Flight 04 in plume rise calculations with PRISM significantly improved the plume height estimates.

Table S1. Statistical comparison of average monthly SO_2 surface concentrations against WBEA continuous monitoring data with GM-orig and GM-PRISM (with $\rho_{conv} = 0.1\%$) simulations for the period from February to July 2018. **R** is the correlation coefficient, **FAC2** is the fraction of predictions within a factor of 2 of observations, **NMB** is the normalized mean bias, and **RMSE** is the root mean squared error. Note that the results presented here are from GEM-MACH model runs driven by a previous version of the emissions input data (which lacked variable CEMS stack parameters and water emissions from several stacks) compared to the results presented in the main text. These results are included in the supplementary document to demonstrate the impact of different ρ_{conv} values on model outcomes.

	Summertime		Wintertime		Full 6-month	
Statistics	GM-orig	GM-PRISM	GM-orig	GM-PRISM	GM-orig	GM-PRISM
R	0.78	0.78	0.70	0.64	0.70	0.69
FAC2	0.73	0.71	0.90	0.68	0.82	0.70
NMB	-0.42	-0.27	-0.19	-0.42	-0.30	-0.35
RMSE	0.52	0.42	0.43	0.57	0.48	0.50

Table S2. Statistical comparison of average monthly SO_2 surface concentrations against WBEA continuous monitoring data with GM-orig and GM-PRISM (with $\rho_{conv} = 0.3\%$) simulations for the period from February to July 2018. **R** is the correlation coefficient, **FAC2** is the fraction of predictions within a factor of 2 of observations, **NMB** is the normalized mean bias, and **RMSE** is the root mean squared error. Note that the results presented here are from GEM-MACH model runs driven by a previous version of the emissions input data (which lacked variable CEMS stack parameters and water emissions from several stacks) compared to the results presented in the main text. These results are included in the supplementary document to demonstrate the impact of different ρ_{conv} values on model outcomes.

	Summertime		Wintertime		Full 6-month	
Statistics	GM-orig	GM-PRISM	GM-orig	GM-PRISM	GM-orig	GM-PRISM
R	0.78	0.80	0.70	0.57	0.70	0.69
FAC2	0.73	0.84	0.90	0.63	0.82	0.74
NMB	-0.42	-0.06	-0.19	-0.16	-0.30	-0.11
RMSE	0.52	0.45	0.43	0.57	0.48	0.52

Table S3. Statistical comparison of average monthly SO_2 surface concentrations against WBEA continuous monitoring data with GM-orig and GM-PRISM (with $\rho_{conv} = 0.5\%$) simulations for the period from February to July 2018. **R** is the correlation coefficient, **FAC2** is the fraction of predictions within a factor of 2 of observations, **NMB** is the normalized mean bias, and **RMSE** is the root mean squared error. Note that the results presented here are from GEM-MACH model runs driven by a previous version of the emissions input data (which lacked variable CEMS stack parameters and water emissions from several stacks) compared to the results presented in the main text. These results are included in the supplementary document to demonstrate the impact of different ρ_{conv} values on model outcomes.

	Summertime		Wintertime		Full 6-month	
Statistics	GM-orig	GM-PRISM	GM-orig	GM-PRISM	GM-orig	GM-PRISM
R	0.78	0.80	0.70	0.67	0.70	0.73
FAC2	0.73	0.79	0.90	0.73	0.82	0.76
NMB	-0.42	0.17	-0.19	0.54	-0.30	0.37
RMSE	0.52	0.66	0.43	1.07	0.48	0.89

References

Briggs, G. A.: Plume Rise Predictions," Lectures on Air Pollution and Environmental Impact Analyses, Workshop Proceedings, American Meteorological Society, Boston, MA, USA, pp. 59–111, 1975.

Iribarne, J. V. and Godson, W. L.: Atmospheric Thermodynamics, 1981.

Oxford: A Dictionary of Statistics (last acess: 20 Decembre 2024), Oxford University Press, https://doi.org/10.1093/acref/9780199679188.001.0001, https://www.oxfordreference.com/view/10.1093/acref/9780199679188.001.0001/acref-9780199679188, 2014.

Rogers, R. R. and Yau, M. K.: A Short Course in Cloud Physics, 1989.